SMGroup

Intracranial Cavernomas and Gamma Knife Radiosurgery

Hakan Kayali*

Department of Neurosurgery, İbn-i Sina Hospital, Turkey

*Corresponding author: Hakan Kayali, Department of Neurosurgery, İbn-i Sina Hospital, Maresal Fevzi Cakmak Mh. Musa Sahin Bulvari No:2, Osmaniye, Turkey, Email: hakankayali@hotmail.com

ABSTRACT

Microsurgical resection, stereotactic radiosurgery (SRS), and conservative management are three methods of treatment for intracranial cavernomas. However if left untreated, cavernomas may lead to intracerebral hemorrhage, seizures, focal neurologic deficits, or headaches. Deciding how to manage a cavernoma patient depends on a multitude factors. While microsurgery is the standard treatment for intracranial cavernomas, conservative treatment should be the choice for the patients without new or progressive neurological deficits and two or more documented hemorrhages and with seizure responsive to the medical treatment. For the others the treatment is primarily surgical for the cases with non-eloquent locations and the results have been best where complete excisions is achieved.

Radiosurgery, especially Gamma Knife (GK) usage is an important alternative for treatment of deep and eloquent area located cavernomas and for the patients who do not accept surgical treatment.

Keywords: Cavernoma; Cerebral; Gamma knife; Radiosurgery.

INTRODUCTION

Cavernomas (cavernous malformations, cavernous angiomas, angiographically occult vascular malformations) are congenital vascular anomalies of the brain. Their recognition as incidental or symtomatic vascular malformations has been facilitated by Magnetic Resonance (MR) imaging. Cavernoma is a benign vascular hamartoma. Multiple lesions are reported in 8 to 18 % of cases. Multiple cavernomas are common in the South-western part of the United States among Hispanic patients. Familial incidence is reported in 50 % of multiple cavernomas and an autosomal dominant inheritance with variable penetrance is suspected. There is no convincing hereditary link with single lesions. They can be located in any brain region, be of varying size, and present with different clinical disorders. About 75 % of the lesions are located in the supratentorial region (1/4 in the frontal and 1/6 in the temporal lobes) and 25% in the infratentorial region (50% in the pons or brainstem). There is no sex prevalence and most symptoatic cases are found between 20-40 years old [1]. Histopathologically, they are characterized by dilated thin walled vascular channels lined by a simple endothelium and thin fibrous adventitia; typically, no brain parenchyma is found within lesion [2]. They rarely occur in the spinal cord [3,4].

Etiology

The etiology of cavernomas is unknown. Cranial radiation, coexistent vascular malformation, genetic, and hormonal factors all have been implicated for the cavernomas. The proportion of patients developing clinical symptoms is higher in the hereditary form than in the sporadic form of the cavernoma [5,6]. De novo formation of cavernoma during immunosuppressive treatment has also been reported. There are some radiation-induced cavernomas occurring in childhood and adolescence [7,8]. Approximately 40-60% of patients with cavernomas have the familial form, inherited in an autosomal dominant pattern due to a heterozygous mutation in one of three genes, CCM1, CCM2, and CCM3, found on the 7q, 7p, and 3p chromosomes, respectively [9]. The familial form usually results in multiple cavernomas, whereas the sporadic disease typically leads to a single cavernoma [10,11]. The products of the cavernoma genes have been shown to play a major role in angiogenesis by associating with cytoskeletal and interendothelial cell junction proteins in neural tissue [12]. Loss-of-function mutations in one of these genes disrupt the endothelial cell-cell junctions, leading to extensive vascular abnormalities and increased permeability.

Epidemiology

Cavernoma of the brain is found in 0.1 % to 4 % of all vascular malformations of the brain. In 4,068 cases of prospective autopsy study, McCormick identified cavernoma in 0,4 %, artriovenous malformations in 0,6 % telengiectases in 0,7 % and venous malformations in 2,6 % [13].

Pathology

Cavernoma consists of a group of thin walled vessels as discrete, lobular and well circumscribed lesions inside the parenchyma of the brain. Grossly it appears as a raspberry-like lesion red

purple in colour. Microscopically it consists of dilated thin walled capillaries with variable thin fibrous adventitia devoid of smooth muscle and elastin. There is no brain parenchyma between the vascular channels. Hemosiderin deposits are always present inside the surrounding normal parenchyma indicating that diapedesis of red blood cells is a common event in all cavernomas [14] (Figure 1).
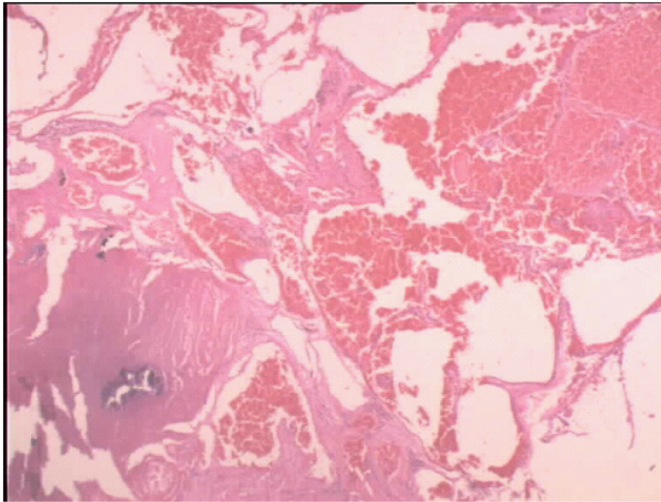

Figure 1: Microscopically cavernoma consists of dilated thin walled capillaries with variable thin fibrous adventitia devoid of smooth muscle and elastin. There is no brain parenchyma between the vascular channels. Hemosiderin deposits are always present inside the surrounding normal parenchyma indicating that diapedesis of red blood cells is a common event in all cavernomas.

CLINICAL PRESENTATION

Epilepsy

Seizures are the most frequent clinical presentation of supratentorial cavernomas, occuring in 41 % to 80 % of patients in this group is estimated to be 1,3 % to 2,8 %. Seizure incidence is two-to-five times higher compared to patients suffering from epilepsy. High epileptogenicity is probably due to perifocal changes in adjacent brain parenchyma. Typical of cavernoma, perifocal collection of blood breakdown products combined with inflammatory alterations and gliotic changes seems to be an organic substrate of epileptogenicity in these patients [15]. Iron ions have a role in producing free radicals and lipid peroxides, which affect functioning of certain cell receptors. The subsequent cascade of changes includes a marked increase in excitatory neurotransmitter amino acids [16]. Such activation has also been discoverd in electrophysiological studies, which have shown more than twice the value in higher evoked activity in cavernoma-neighboring neurons than in cells around glial tumors [17].

Hemorrhage

An *intralesional (or encapsulated) hemorrhage* is limited to the border of the lesion and causes enlargement of the cavernoma. It is likely that the surrounding hemosiderotic parenchyma, which is strengthened by gliosis, takes a role in preventing the hemorrhage from spreading outside into healthy parenchyma. This can lead to formation of a capsule, which behaves like the membrane of a chronic subdural hematoma, osmotically attracting fuild and leading to enlargement of the cavernoma. A weakened capsule with hemodynamic stress is a possible factor predisposing to more prominent bleeding, which invades nearby brain areas.

An *extralesional (or overt, gross) hemorrhage* extends beyond the hemosiderotic ring and on MRI shows signs of acute or subacute bleeding. This "true" intracerebral bleeding can cause marked disruption of surrounding tissue and lead to permanent deficits depending on the location.

Both intralesional and extralesional hemorrhages usually manifest with acute onset of headaches accompanied by focal deficit or seizures.

Early series showed hemorrhage incidence in cavernoma patients to be up to 65 %. However, most of the studies were influenced by significant patient selection bias and mixing of different pathological entities; as a rule, patients were investigated after acute symptoms and hemorrhage and could have even had an arteriovenous malformation, which carries a higher risk of profuse hemorrhage than a cavernoma. In more recent studies based on MRI findings with recruited asymptomatic patients. The extralesional hemorrhage rate appears to be low, on average 1 % per patient-year (range: 0.25-2,5 %). In familial cases, bleeding rates may vary depending on the cavernoma genotype. Notably, Denier et al. in 2006 found that carriers of CCM3 are more prone than patients with CCM2 and CCM1 to develop cerebral hemorrhages, especially at a younger age [18].

Hemorrhage in patients with multiple cavernomas is not uncommon, as up to 32 % of patients present with hemorrhage. The annual rate of bleeding ranges from 0.25 % to 16.5 % per patient-year or, if considering the mean number of lesions in one person, 0.1 % per lesion-year to 22.5 % per lesion-year. Labauge et-al. in their retrospective study measured that supratentorial cavernomas bled at rate of 1.9 % per lesion-year [19].

Lesions in the infratentorial compartment and particularly the brainstem are characterized by higher bleeding rates than their supratentorial counterparts, ranging from 2.5 % per patient-year to 5 % per patient-year. Interestingly, larger lesion size (>1cm), early age at presentation (<35 years), and coexistence of a developmental venous anomaly were found to be associated with higher hemorrhage rates [20].

Focal neurologic deficits

The apperance of focal neurologic deficits in cavernoma patients is not uncommon when

lesions affect the motor cortex, speech areas, basal ganglia and brainstem. Kayali et-al reported imbalance 19 %, hemiparesis 13 %, speech disorder 11 %, dismetri 8 %, impairment of vision 5 %, hearing loss 5 %, tremor 5 % in analysis of 37 intracranial cavernoma cases in 2004 [21].

Radiological characteristics

According to Mouchtouris and co-workers' report [22]; the diagnosis of cavernomas is more difficult than other vascular diseases since cavernomas are angiographically occult malformations. Angiography is only able to detect the existence of abnormal venous drainage associated with cavernomas; thus other imaging techniques are needed to provide an accurate diagnosis. Conventional T1- and T2-weighted MR imaging, gradient echo sequences, high-field MRI, susceptibility-weighted imaging, diffusion tensor imaging, and functional MRI are some of the advanced techniques that are being used for diagnosis of cavernomas or for intraoperative navigation during the treatment of deeply located lesions [22].

CONVENTIONAL T1- AND T2 WEIGHTED MR IMAGING

Conventional MR imaging is able to accurately detect symptomatic cavernous malformations, which are surrounded by a ring of hypointensity due to hemosiderin deposits from recurring microhemorrhages [23,24]. The CM lesions are divided into four types based on their appearance on MR imaging.

Type I lesions: Appear hyperintense on T1- and T2-weighted imaging due to a hemosiderin core from subacute hemorrhage (Figure 2).
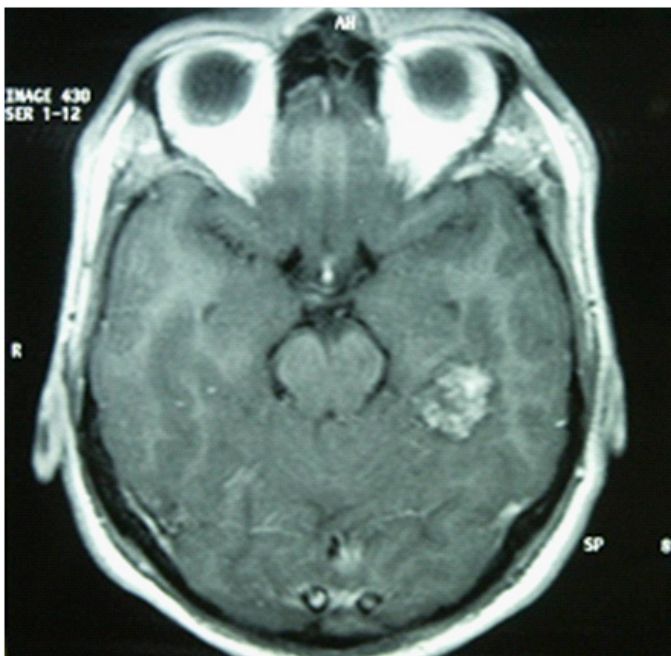

Figure 2: Type I lesions appear hyperintense on T1- and T2-weighted imaging due to a hemosiderin core from subacute hemorrhage.

Type II lesions: Contain loculated hemorrhages enveloped by gliotic tissue, presenting as a mixed signal on both T1 and T2 sequences. On T2 imaging, type II lesions also have a hypointense rim, resulting in the "popcorn" appearance [25] (Figure 3).

Figure 3: Type II lesions contain loculated hemorrhages enveloped by gliotic tissue, presenting as a mixed signal on both T1 and T2 sequences. On T2 imaging, type II lesions also have a hypointense rim, resulting in the "popcorn" appearance.

Type III lesions: Are diagnosed by the presence of an isointense core, indicating chronic resolved hemorrhage, typically seen in familial CM.

Type IV lesions: Are small malformations that can only be seen in Gradient Recalled Echo (GRE) MRI as hypointense foci and are thought to be capillary telangiectasias [24, 26].

GRADIENT RECALLED ECHO (GRE) MR IMAGING

GRE MR imaging is a key method for diagnosis of cavernomas due to its ability to display hemosiderin-filled brain tissue with a very distinct hypointensity. Studies on familial cavernomas have shown that conventional MR imaging detected an average of 5 lesions per patient, while T2-weighted GRE MRI identified an average of 16 lesions per patient [27]. GRE MRI not only is more capable of identifying all of the lesions present, but also delineates the lesions more precisely [28]. While it has several benefits, it is important to note that GRE MRI augments the apparent size of the CM lesion. Additionally, GRE MR Images may show multifocal lesions in elderly patients

with hypertension and a history of stroke, but they must not be mistaken for familial CMs. They result from hypertensive angiopathy and are located in periventricular areas [23].

USE OF HIGH − FIELD MRI FOR DIAGNOSIS OF CAVERNOMAS

The use of conventional 1.5 T MR imaging is limited, as CM lesions may not be visualized unless high-field MR imaging is used. Using MR strengths of up to 14 Tesla, several studies have illustrated the ability of high-field imaging to visualize lesions as hypointensities that were not otherwise apparent. Depending on the strength, lesions may appear to be larger than in reality. More specifically, high-field imaging at 7 T causes lesions to appear 11% larger than in conventional imaging techniques [29-31].

SUSCEPTIBILITY-WEIGHTED (SW) IMAGING

Susceptibility-Weighted (SW) imaging is very advantageous for detecting CM lesions because it accurately recognizes deoxyhemoglobin and hemosiderin. It is also considered the only method capable of detecting unbled CM lesions and telangiectasias [23]. SW imaging has been shown to delineate CMs more precisely as well as detect additional CM lesions that cannot be seen by conventional imaging methods. De Souza et al. studied 15 patients with familial CMs and found 5.7, 26.3, and 45.6 lesions per patient using T2-weighted imaging, T2 * GRE imaging, and SW imaging, respectively. SW imaging detected 1.7 times more lesions than T2 * GRE (P=0.001) [32]. Other studies on familial CMs corroborate these findings; however, SW imaging is not superior to T2 GRE imaging regarding the detection of sporadic, solitary CMs or clusters of CMs associated with a DVA [23]. Additionally, using sequential SW imaging with contrast agent may prove very useful in distinguishing venous vasculature from small regions of hemorrhage, but this application of SW imaging needs to be studied further [33].

DIFFUSION TENSOR (DT) IMAGING AND FMRI USED INTRAOPERATIVELY

DT and fMR imaging are used intraoperatively to better visualize the lesions and the surrounding parenchyma in order to improve the surgical outcome even if the lesions are deeply located in eloquent areas. DT tractography allows the surgeon to visualize the white matter tracts, which frequently cross through the hemosiderin rim of the CM lesion [25]. Several studies have shown the successful use of DT imaging in locating the tracts and avoiding them, significantly decreasing the morbidity associated with CM resections [34-36]. fMR imaging measures activity-dependent changes in cerebral blood flow, which becomes especially useful when resecting CM lesions located in eloquent brain [37,38]. Zotta et al. show the use of fMRI for surgical planning and intraoperative navigation and report higher rates of completely seizure-free patients. The use of fMRI neuronavigation enabled them to follow a more aggressive approach on the perilesional tissue without increasing the morbidity rate [39].

There is promising evidence supporting the use of DT and fMR imaging intraoperatively to achieve better outcomes without an increase in the morbidity and mortality rates. However,

most studies on the neuronavigation techniques involve only a small number of patients; further investigation of these techniques is warranted using a larger number of patients to ensure generalizability [22].

GAMMA KNIFE RADIOSURGERY

A Brief Historical Review

Professor Lars Leksell first coupled an orthovoltage X-ray tube with his first-generation guiding device to focus radiation on the Gasserian ganglion to treat facial pain. He subsequently investigated cross-fired protons as well as X-rays from an early-generation linear accelerator (linac) for radio surgery. In the 1960s, he became dissatisfied with the cumbersome nature of cross-fired proton beams and the poor reliability and wobble of then-existing linear accelerators. Lexell and Larson finally selected cobalt-60 as the ideal photon radiation source and developed the Gamma Knife. They placed 179 60 Co sources in a hemispherical array so that all gamma rays (radiation from the decay of 60Co focused on a single point there by creating cumulative radiation isocenters of variable volume depending on the beam diameter. The first Gamma Knife created a discoid shaped lesion suitable for neurosurgical treatment of movement disorders and intractable pain management.

Clinical work with the Gamma Knife began in 1967 at the manufacturing site, the Motala AB workshop near Linköping, Sweden. The first patient had a craniopharyngioma. The patient's head was immobilized using a plaster-molded head-piece. In 1975, a series of surgical pioneers at the Karolinska Hospital, Stockholm, began to use a reengineered Gamma Knife (spheroidal lesion) for the treatment of intracranial tumors and vascular malformations. Units 3 and 4 were placed in Buenos Aires and Sheffield England in the early 1980s. Lunsford et al. introduced the first clinical 201-source Gamma Knife unit to North America (the fifth gamma unit worldwide). Lunsford first performed Gamma Knife radiosurgery in August 1987 at University of Pittsburgh Medical Center. In the United States, based on the available published literature, arteriovenous malformations and skull base tumors that failed other treatments were considered the initial indications for radiosurgery. A cautious approach was adopted while waiting for increased scientific documentation. The encouraging results of radiosurgery for benign tumors and vascular malformations led to an exponential rise of radiosurgery cases and sales of radio surgical units. In recent years, metastatic brain tumors have become the most common indication for radiosurgery. Brain metastases now comprise 30 % to 50 % of radiosurgery cases at busy centers [40].

Latest Developments in Gamma Knife Radiosurgery

According to Ceviker and co-workers' report [41], a wide application field, high precision and low complication and high success rates make Gamma Knife radiosurgery a standard treatment modality in neurosurgery. During Gamma Knife radiosurgery, 201 cobalt 60 sources are arranged in a hemispheric shape in such a manner that all the gamma rays are focused at the center to create a cumulative radiation field. The total energy of the rays is therefore transmitted precisely

to the target with preservation of normal brain tissue. The Leksell Gamma Knife has undergone numerous refinements, additions and modifications since 1967. Additions and refinements in Gamma Knife radiosurgery are still continuing parallel to developing technology [41].

Two hundred and one cobalt 60 sources converge and focus on a specific point during stereotactic space Gamma Knife Surgery (GKS). As a result, the target receives a high dose, with a steep fall-off in the dosage gradient peripherally. The principal is to create a high radiation effect on the target while sparing the surrounding structures. As the energy of each ray is very weak, the rays do not cause a significant biological effect on the normal brain tissue that they pass through.

The first applications of Gamma Knife® were performed at the Karolinska Institute (Sweden) by Swedish neurosurgeon Lars Leksell and professor of biophysics Borje Larsson in the early 1950's. They irradiated the Gasserian ganglion of a patient suffering from tic douloureux with a stereotactic frame adapted to a conventional X-ray machine. The prototype of the modern Gamma Knife was produced and used at the same Institute in 1967. It was called Model A or U and there were 179 sources of cobalt 60 in this machine. Since imaging techniques were insufficient, Gamma Knife Surgery (GKS) was mostly used in functional neurosurgery at that time [42- 46]. Thanks to further developments in computer and imaging technologies, GKS was improved and Model B was produced. Model B was installed first in Bergen in Norway. This model is still used in more than 100 centers around the world, and also in the first center in Turkey. Model B makes three-dimensional, complex treatment planning possible by using modern imaging techniques (Computed Tomography (CT), Magnetic Resonance Imaging (MR) and Digital Subtraction Angiography (DSA)). After approval by the FDA (Food and Drug Administration) in 1988, GKS was accepted as a dedicated neurosurgical treatment tool and spread all over the world [46]. There were only 5 centers using GKS in the world in 1988 but this number has now reached 217. It is estimated that more than 250,000 patients have been treated with GKS until 2004. Another leading factor of this progress is the efficiency of GKS in treating Arterio-Venous Malformations (AVM). The use of a shielding system (plugs) is a very important step in GKS. This system blocks the beams passing through eloquent and sensitive structures such as the optic tract and brain stem. Safe treatment with low complication rates can thus be achieved. Gamma Knife evolved parallel to technological developments and Model C was produced in 1999. This model was designed both to reduce the treatment time for radiosurgery and to prevent human errors [47]. The most important feature of this model is the Automatic Positioning System (APS). This system carries the target to the focus automatically according to the treatment plan with very high precision. APS provides fast, safe, more accurate and very precise treatment planning [45,48-51]. Model C can also work without APS. Easy use of the new helmet transport system, color-coded collimators and occlusive plugs are the other advantages of this model. "Gamma Plan" is the computer software used in treatment planning in GKS and is the most intelligent part of the system. Gamma Plan 4C is currently the most advanced such system. Gazi University Gamma Knife Center in Turkey is the first center uses this system in all over the world. This software is capable of using Positron

Emission Tomography (PET) images and involves an integrated electronic Schaltenbrand / Wahren stereotactic brain atlas. It fuses the anatomical structures in the electronic Schaltenbrand / Wahren stereotactic brain atlas images to the patient's images. The third important feature of the software is the capability to use frameless images with the guidance of the framebased images. To the best of our knowledge GKS Units in clinical use worldwide reached 305 until 2013.

GAMMA KNIFE MODEL C

Gamma Knife Model C consists of 6 major separate units. APS is the main difference of Model C from the previous models. The well-known five units of the system are also briefly described below.

Treatment unit

This unit consists of 201 hemispherically-arranged cobalt 60 sources.

Collimators

These are used to define the volume of the radiation field that the beams constitute. For instance, while the 4 mm collimator produces 0.07 ml of active radiation field, the 18 mm collimator produces 6 ml active radiation field [50]. There are four different collimator sizes (4,8,14,18 mm) that are chosen according to the lesion's shape, size and localization. The hemispheric tool containing the 201 collimators is called the "helmet".

Patient Couch

This is the bed that the patient lies on and which automatically moves in and out of the treatment unit.

Leksell Stereotactic Frame

This is used to define the coordinates of any structure in the cranium. It also ensures immobility of the patient's head during the imaging and treatment procedures. The frame is attached to the skull under local anesthesia by four head pins. The Leksell frame must be placed so that the target is located as close to the center of the frame (x:100, y:100, z:100) as possible. Sometimes lesions placed in frontal poles, occipital poles or lateral poles cannot be centralized and treatment cannot be performed in these situations.

Planning System (Gamma Plan)

After the application of the frame, images are transferred to the planning system. By the help of fiducials (indicators with coordinates already installed in the software), the coordinates of the target are recognized by the computer. The operator defines and introduces the target to the computer by drawing the margins of the lesion. The lesion is then covered with shots. These shots produce isocenters that can roughly be defined as active radiation fields. Gamma Plan also predicts any collisions (hit) of the patient's head and the frame to the helmet before the

treatment and warns the operator. Once the treatment plan is completed, the plan is exported via the network to the treatment control console computer. After positioning the patient on the couch, a second check is carried out by the operators called 'collision and position check run.

Automatic Positioning System (APS)

GKS usually involves multiple isocenters to achieve a treatment plan that conforms to the irregular three dimensional volumes of most lesions. The APS moves the patient's head to the target coordinates defined in the treatment plan. In other words, this system adjusts the stereotactic coordinates of isocenters automatically. Robotic movement is performed by the six positioners (each directing one axis; X,Y,Z) located on the left and right side of the head. In the APS, the movements and coordinates are checked by another system 10 times a second, thus providing a high degree of accuracy and safety. Coordinate adjustment was performed manually with the system called "Trunnion" in previous models. Operators had to enter the treatment room and adjust the coordinates manually for every shot in Model B. The robot eliminates the time spent for removing the patient from the helmet, setting up the new coordinates for each isocenter using the same beam diameter, and repositioning the patient in the helmet. The time required to complete the treatment is therefore reduced significantly. Since the aim of stereotactic radiosurgery is to design and implement a treatment plan in which the prescription isodose line covers the target with a minimal excess volume and a sharp dose fall-off outside the target volume, the shortened treatment time helps to create a more precise three-dimensional plan by using multiple small isocenters [47-50]. A sharp dose fall-off outside the target volume means high selectivity and lower complication rates. In stereotactic radio surgery, the term "conformality" is used to define how much or what percentage of the target is covered by the isodose line and "selectivity" is used to define how well the isodose line fits the target shape. Horstmann et al compared patients with vestibular schwannoma who were treated with and without APS. They reported that APS provides more conformal and selective treatment plans [48]. In a similar study, Regis et al reported that the total treatment time was reduced by %53 and that conformity and selectivity were improved from 95% to 97% and 78% to 84% respectively in the treatment of vestibular schwannomas [50]. Model U and C were compared in the treatment of cavernous sinus meningiomas [49]. Kuo et al. reported higher conformality, shorter treatment time (approximately 1 hour) and lower radiation dose in the optic chiasm (3.8 Gy and 5.3 Gy respectively) with Model C [49]. Another important advantage of APS is the elimination of errors in setting stereotactic coordinates manually. Flickinger et al found an error rate of 8% in setting the coordinates (for errors between 0.25 and 0.5 mm) before the second check. This number was reduced to 1 in 1392 after checks by two independent observers [52]. APS sets the coordinates more accurately than the manual procedure since the system is sensitive to 0.1 mm. Model C and APS also provide lower radiation dose delivery to the operators and the extra cranial regions of the patient [53]. The patient couch automatically withdraws the patient 28 cm from the radiation focus between the shots to minimize unplanned radiation delivery. Kondziolka et al. measured the sternal and

gonadal dose fall-offs for trunnion and APS by using phantom. They reported lower radiation fall-off in sternal and gonadal regions with APS for the same treatment [53]. As the operators enter the treatment room less frequently in Model C, they do not receive significant radiation [47]. There are two limiting factors for APS use: extreme coordinate locations and patients with broad shoulders and short necks. Far lateral lesions (>40 mm from the midline of the frame) and inferior targets (lower than the level of pons) may not be reached in some cases [53]. Treatment cannot be performed in these situations. APS positioners are located on each side of the head and just above the shoulders. Sometimes it may not be possible to place the patient's head to the APS because the broad shoulders can hit the positioners. Ceviker et-al. prefers to treat the patient with the trunnion mode in such cases.

GAMMA PLAN 4C

Gamma Plan is the software used in treatment planning. The latest version is Gamma Plan 4C and it has important advantages to previous versions. The latest technological developments are used in this software. Gazi University Gamma Knife Center in Turkey is the first center to use Gamma Plan 4C in the world. The three main features of Gamma Plan 4C are listed below:

1. Planning with stereotactic PET images.

2. Integrated electronic Schaltenbrand / Wahren stereotactic brain atlas.

3. Capability to use frameless images.

Another feature of the software is the system called "wizard". The last two versions have the wizard that is used to cover the target with shots automatically. It is thought that this system cannot be used alone for planning but it can be help the operator in some conditions. PET is used to evaluate the extent and degree of anaplasia and the prognosis via the metabolic activity of the tumor. It has limited use for determining anatomical details. Efficiency of PET images in stereotactic brain biopsies is the background of the contribution of PET images to stereotactic radiosurgery [54-57]. Integration of PET to neurosurgical procedures may contribute to a better management of brain tumors, either by optimizing their delineation or by targeting the true aggressive areas of heterogeneous tumors. MR and CT do not provide sufficient data for the true margins of invasive tumors. They also have limited use in the differential diagnosis of tumor recurrences and radio necrosis in some cases. These cases constitute a big problem for the surgeon since target definition is vital for stereotactic radiosurgery. The contribution of PET images can be helpful for better planning in such cases. In 2004, Levivier et al treated 57 patients with GKS using MR and PET images at the same time. The authors integrated PET because the tumor margins were not well-defined in MRI. They found 86% abnormal PET uptake and this information altered the MRI-defined tumor significantly in 69% of the targets [58]. The integrated electronic Schaltenbrand / Wahren stereotactic brain atlas is the second important feature of the Gamma Plan 4C. After introducing the AC-PC line to the computer and defining the midline, the software shows any

structure of patient brain that the operator wants to see. The coordinates of these structures can also be obtained. GKS is accepted as a safe and effective way of treatment in functional neurosurgery [59,60]. Ceviker et-al. believe that this atlas has great advantages not only in functional stereotactic radiosurgery but also for safer treatment of tumors and AVM's that are located in basal ganglia's. The third advantage of the new version is the capability of using non-frame based images by fusing these images to frame-based images. Gamma Plan 4C enables co-registration of non-stereotactic tomographic data (MR, CT, PET) to a frame-based study for the same patient. Frame-based images act as a guide for this process. This feature helps to compare the images objectively on follow-ups and prevent unnecessary repetitions of CT, MR or PET scans.

OUTCOMES AFTER GAMMA KNIFE SURGERY IN CAVERNOMAS

Some authors have found that there was no difference in the hemorrhage rate before and after GKS [61]. However, other authors suggested that it could be performed for eloquent sites [62-64]. Hasegawa et al. reported that the annual hemorrhage rate was 12.3% for the first 2 years after radiosurgery and 0.8% thereafter [65]. Another study by Kida and Hasegawa has reported that the bleeding rate was 8% at 1st year after radiosurgery, 5% in the 2nd year and 0% by year 7 [66]. Other studies have shown annual hemorrhage rates of 3.3–9.4% for the first several years after GKS and then lower hemorrhage rates in later years of follow-up [67-73].

Previously reported mean rates of the volume reduction after radiosurgery for CMs varied from 37.3% [74] to 81% [75]. These are similar to Parisa Azimi et-al. findings. However, it is unclear whether shrinkage of the bulk is really induced by radiation or other factors and needs to be investigated in the future [76].

The optimal dose of CMs for a positive response and minimum side effects is controversial. Liscák et al. showed statistically significant increases in the collateral edema by marginal dose exceeding 15 Gy [61]. Lee et al. reported that radiation-related complication developed with marginal dose 13 Gy, and they suggested that lower radio surgical doses are required for CMs in specific sites such as brainstem [74]. Similar finding was reported by Amin-Hanjani et al. and Karlsson and Tsai [77,78]. Pariza Asimi et-al. also recommends low-dose radiosurgery using on average a 13 Gy marginal dose [76].

On the other hand, Kayali et-al. performed X-knife radio surgery for 13 cavernoma patients between 1995-2003 in Department of Neurosurgery School of Medicine, Gülhane Military Medical Academy (GMMA), and Ankara in Turkey. In radio surgical treatment, Linear Accelerator (Philips SL-25, UK), Isocentric subsystem (Philips K-X 200, UK), Brown-Roberts-Wells Head Frame (Radionics Co., USA) and X knife3 planning system (Radiosonics Software Applications Inc., USA) were used. 6 MeV X-ray was produced by Linear Accelerator. In all cases single isocenter, median 310 degree total arch angle (300-320) and median 6 arch (5-7) were used. Median 15 Gy (14-20) was applied to the peripheral zone of the lesion (80%). The results were uneventful except for

one underwent microsurgery due to increased seizure frequency. Hemorrhage, edema around the lesions and increase in the size of the lesions were not observed in the patients treated radio surgically up to date [21] (Figure 4).
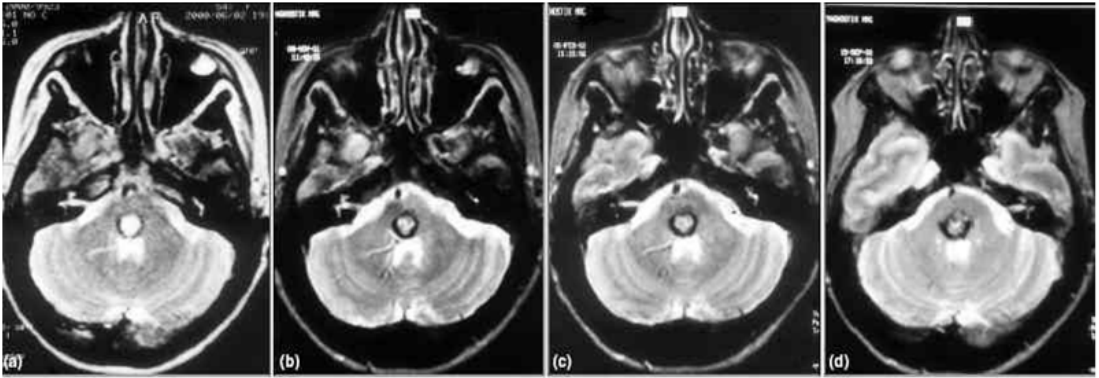

Figure 4: T2 weighted axial MRIs of a cavernoma is located brainstem, treated by using X-knife radiosurgery

(a) before the radiosurgery (b) 6th month after radiosurgery (c) 9th month after radiosurgery and (d) 16th month after radiosurgery.

The important criterias of a succesfull radiosurgery are there is no edema around the lesion, no increase in size of the lesion and there is no bleeding after radiosurgery.

To the best of our knowledge the treatment of intracranial cavernomas with radio surgery first began with this X-knife radiosurgery in Turkey by Department of Neurosurgery of GMMA and the results were presented in 18th Annual Meeting of Turkish Neurosurgical Society in 2004. After this presentation the other universities have begun to use Gamma Knife Radiosurgery for intracranial cavernomas in Turkey. Technically, when compared with X-knife, the superiority of Gamma Knife is unquestionable, so Gamma Knife is an important option in treatment of intracranial cavernomas.

Kida et-al. reported a multi-institutional retrospective study in Japan in 2015. A total of 298 cases collected from 23 GK centers across Japan were icluded. 173 males and 125 females patients ranging in age from 7 to 73 years were treated with gamma knife from 1991 to 2012, and with a sufficient follow-up period at least more than 12 months. In this study hemorrhage was the most common manifestation, followed by seizures and neurological deficits. Most of the lesions were located in the brainstem and basal ganglia, followed by the cerebral or cerebellar hemispheres. The cavernomas which had a mean diameter of 14.8 mm were treated using GK surgery with a mean marginal dose of 14.6 Gy. Superficial cavernomas located cerebellum or lobar regions responded to the treatment better than deeply located cavernomas in the basal ganglia or brainstem. No significant difference of dose-dependent response was seen for three different ranges of marginal dose: Less than 15 Gy, between 15 and 20 Gy, and more than 20

Gy. Complications were more frequent after a marginal dose over 15 Gy and in patients with lesions more than 15 mm in diameter. The rates of annual hemorrhage were estimated to be 7.4 % during the first 2 years after radiosurgery and 2.8 % thereafter. The overall hemorrhage rate after radiosurgery was 4.4 % / year/ patient in this study. They concluded that, because symptomatic cavernomas often show aggressive behaviors, adequate treatment is necessary. After radiosurgery, the annual hemorrhage rate is significantly lower than conservative treatment. GK radiosurgery is an important option, since the adverse effects are less frequent than with surgery, especially for eloquent locations such as the brainstem or basal ganglia. Radiosurgery brings the hemorrhage rate of these lesions at least to that of natural history when safe doses are used [79].

CONCLUSION

Conservative treatment for intracranial cavernomas should be the choice for the patients without new or progressive neurological deficits and two or more documented hemorrhages and with seizure responsive to the medical treatment. For the others, the treatment is primarily surgical for the cases with non-eloquent locations and the results have been best where complete excision is achieved.

Gamma Knife Surgery has undergone numerous refinements, additions and modifications in recent years. Gamma Knife Model C and Gamma Plan 4C have significant advantages over earlier models. Efficient dose plans which allow treatment using more isocenters with smaller collimators, short treatment time, elimination of human errors in setting the coordinates, lower radiation dose for extracranial compartments and operators are the advantages of Gamma Knife Model C. Gamma Plan 4C provides more accurate target definition by using PET and the Schaltenbrand / Wahren stereotactic brain atlas [41].

Radiosurgery, especially Gamma Knife Radiosurgery is an important alternative for treatment of deep and eloquent area located intracranial cavernomas and for the patients who do not accept surgical treatment.

References

1. Kivelev J, Niemelä M, Kivisaari R, Dashti R, Laakso A, Hernesniemi J. Long-term outcome of patients with multiple cerebral cavernous malformations. Neurosurgery. 2009; 65: 450-455.

2. Kondziolka D, Lunsford LD, Kestle JR. The natural history of cerebral cavernous malformations. J Neurosurg. 1995; 83: 820-824.

3. Cosgrove GR, Bertrand G, Fontaine S, Robitaille Y, Melanson D. Cavernous angiomas of the spinal cord. J Neurosurg. 1988; 68: 31-36.

4. Anand S, Puri V, Sinha S, Malhotra V. Intramedullary cavernous haemangioma. Neurol India. 2001; 49: 401-403.

5. Hayman LA, Evans RA, Ferrell RE, Fahr LM, Ostrow P, Riccardi VM. Familial cavernous angiomas: natural history and genetic study over a 5-year period. Am J Med Genet. 1982; 11: 147-160.

6. Robinson JR, Awald IA. Clinical spectrum and natural course. Awald IA, Barrow DI, editors. In: Cavernous malformations. Park Ridge, III: American Association of Neurological Surgeons. 1993; 25-36.

7. Brunken M, Sagehorn S, Leppien A, Müller-Jensen A, Halves E. [De novo formation of a cavernoma in association with a preformed venous malformation during immunosuppressive treatment]. Zentralbl Neurochir. 1999; 60: 81-85.

8. Amirjamshidi A, Abbassioun K. Radiation-induced tumors of the central nervous system occurring in childhood and adolescence. Four unusual lesions in three patients and a review of the literature. Childs Nerv Syst. 2000; 16: 390-397.

9. Dalyai RT, Ghobrial G, Awad I, Tjoumakaris S, Gonzalez LF, Dumont AS, et al. Management of incidental cavernous malformations: a review. Neurosurg Focus. 2011; 31: E5.

10. Zabramski JM, Wascher TM, Spetzler RF, Johnson B, Golfinos J, Drayer BP, et al. The natural history of familial cavernous malformations: results of an ongoing study. J Neurosurg. 1994; 80: 422-432.

11. Laberge-le Couteulx S, Jung HH, Labauge P, Houtteville JP, Lescoat C, Cecillon M, et al. Truncating mutations in CCM1, encoding KRIT1, cause hereditary cavernous angiomas. Nat Genet. 1999; 23: 189-193.

12. Yadla S, Jabbour PM, Shenkar R, Shi C, Campbell PG, Awad IA. Cerebral cavernous malformations as a disease of vascular permeability: from bench tobedside with caution. Neurosurgical focus. 2010; 29: E4.

13. McCormick WF. The pathology of vascular ("arteriovenous") malformations. J Neurosurg. 1966; 24: 807-816.

14. Ching-fai Fung. Cavernous Haemangioma of Brain. The Hong Kong Medical Diary. 2011; 16: 14-16.

15. Awad I, Jabbour P. Cerebral cavernous malformations and epilepsy. Neurosurg Focus. 2006; 21: e7.

16. von Essen C, Rydenhag B, Nyström B, Mozzi R, van Gelder N, Hamberger A. High levels of glycine and serine as a cause of the seizure symptoms of cavernous angiomas? J Neurochem. 1996; 67: 260-264.

17. Williamson A, Patrylo PR, Lee S, Spencer DD. Physiology of human cortical neurons adjacent to cavernous malformations and tumors. Epilepsia. 2003; 44: 1413-1419.

18. Denier C, Labauge P, Bergametti F, Marchelli F, Riant F, Arnoult M, et al. Genotype-phenotype correlations in cerebral cavernous malformations patients. Ann Neurol. 2006; 60: 550-556.

19. Labauge P, Brunereau L, Lévy C, Laberge S, Houtteville JP. The natural history of familial cerebral cavernomas: a retrospective MRI study of 40 patients. Neuroradiology. 2000; 42: 327-332.

20. Kupersmith MJ, Kalish H, Epstein F, Yu G, Berenstein A, Woo H, et al. Natural history of brainstem cavernous malformations. Neurosurgery. 2001; 48: 47-53.

21. Kayali H, Sait S, Serdar K, Kaan O, Ilker S, Erdener T. Intracranial cavernomas: analysis of 37 cases and literature review. Neurol India. 2004; 52: 439-442.

22. Mouchtouris N, Chalouhi N, Chitale A, Starke RM, Tjoumakaris SI, Rosenwasser RHet al. Management of Cerebral Cavernous Malformations: From Diagnosis to Treatment. The Scientific World Journal. 2015; 1-8.

23. Campbell PG, Jabbour P, Yadla S, Awad IA. Emerging clinical imaging techniques for cerebral cavernous malformations: a systematic review. Neurological Focus. 2010; 29: 1-8.

24. Rivera PP, Willinsky RA, Porter PJ. Intracranial cavernous malformations. Neuroimaging Clin N Am. 2003; 13: 27-40.

25. Cauley KA, Andrews T, Gonyea JV, Filippi CG. Magnetic resonance diffusion tensor imaging and tractography of intracranial cavernous malformations: preliminary observations and characterization of the hemosiderin rim. Journal of Neurosurgery. 2010; 112: 814-823.

26. Maraire JN, Awad IA. Intracranial cavernous malformations: lesion behavior and management strategies. Neurosurgery. 1995; 37: 591-605.

27. Labague P, Laberge S, Brunereau L, Levy C, Tournier-Lasserve E. Hereditary cerebral cavernous angiomas: clinical and genetic features in 57 French families. The Lancet. 1998; 352: 1892-1897.

28. Lenhardt FG, Von Smekal U, Rückriem B, Stenzel W, Neveling M, Heiss WD, et-al. Value of gradient-echo magnetic resonance-imaging in the diagnosis of familial cerebral cavernous malformation. Archives of Neurology. 2005; 62: 653-658.

29. Damman P, Barth M, Zhu Y, Maderwald S, Schlamann M, Ladd ME, et al. Susceptibility weighted magnetic resonance imaging of cerebral cavernous malformations: prospects, drawbacks, and first experience at ultra – high field strength (7-Tesla) magnetic resonanse imaging. Neurosurgical Focus. 2010; 29: E5.

30. Novak V, Chowdhary A, Abduljalil A, Novak P, Chakeres D. Venous cavernoma at 8 Tesla MRI. Magn Reson Imaging. 2003; 21: 1087-1089.

31. Schlamann M, Maderwald S, Becker W, Kraff O, Theysohn JM, Mueller O, et al. Cerebral cavernous hemangiomas at 7 Tesla: initial experience. Acad Radiol. 2010; 17: 3-6.

32. de Souza JM, Domingues RC, Cruz LC Jr, Domingues FS, Iasbeck T, Gasparetto EL. Susceptibility – weighted imaging for the evaluation of patients with familial cerebral cavernous malformations: a comparison with T2- weighted fast spin-echo and gradient-echo sequences. The American Journal of Neuroradiology. 2008; 29:154-158.

33. Lin W, Mukherjee P, An H, Yu Y, Wang Y, Vo K, et al. Improving high-resolution MR bold venographic imaging using a T1 reducing contrast agent. J Magn Reson Imaging. 1999; 10: 118-123.

34. Niizuma K, Fujimura M, Kumabe T, Higano S, Tominaga T. Surgical treatment of paraventricular cavernous angioma: fibre tracking for visualizing the corticospinal tract and determining surgical approach. Journal of Clinical Neuroscience. 2006; 13: 1028-1032.

35. Chen X, Weigel D, Ganslandt O, Buchfelder M, Nimsky C. Diffusion tensor imaging and white matter tractography in patients with brainstem lesions. Acta Neurochir (Wien). 2007; 149: 1117-1131.

36. Chen X, Weigel D, Ganslandt O, Fahlbush R, Buchfelder M, Nimsky C. Diffusion tensor-based fiber tracking and intraoperative neuronavigation fort he resection of brainstem cavernous angioma. Surgical Neurology. 2007; 68: 285-291.

37. Schlosser MJ, McCarthy G, Fulbright RK, Gore JC, Awad IA. Cerebral vascular malformations adjacent to sensorimotor and visual cortex: functional magnetic resonance imaging studies before and after therapeutic intervention. Stroke. 1997; vol. 28, no. 6, 1130-1137.

38. Thickbroom GW, Byrnes ML, Morris IT, Fallon MJ, Knuckey NW, Mastaglia FL. Functional MRI near vascular anomalies: comparison of cavernoma and arteriovenous malformation. Journal of Clinical Neuroscience. 2004; 11: 845-848.

39. Zotta D, Di Rienzo A, Scogna A, Ricci A, Ricci G, Galzio RJ. Supratentorial cavernomas in eloquent brain areas: Application of neuronavigation and functional MRI in operative planning. Journal of Neurosurgical Sciences. 2005; 49: 13-19.

40. Niranjan A, Sirin S, Flickinger JC, Maitz A, Kondziolka D. Gamma Knife Radio surgery, Principles and Practice of Stereotactic Radio surgery. 2008; 107-127.

41. Ceviker N, Pasaoglu A, Akyol S, Orbay T. Latest Developments in Gamma Knife Radiosurgery: Gamma Knife Model C and Gamma Plan 4C. Turkish Neurosurgery. 2005; 15: 52-57.

42. Kiliç T, Peker S, Pamir MN. Gamma Knife ® Isin Cerrahisi: Teknigi, Endikasyonlari, Sonuçlari, Sinirlari. (Gamma Knife ® Ray Surgery: Technique, Indications, Results, Limitations) Türk Nörosirurji Dergisi. 2000; 10: 119-136.

43. Lindquist C, Kihlström L, Hellstrand E. Functional neurosurgery--a future for the gamma knife? Stereotact Funct Neurosurg. 1991; 57: 72-81.

44. Lunsford LD, Kondziolka D, Flickinger JC. Stereotactic radiosurgery: current spectrum and results. Clin Neurosurg. 1992; 38: 405-444.

45. Niranjan A, Kondziolka D, Maitz AH, Lunsford LD. Radiosurgery: current techniques. Tech in Neurosurg. 2003; 9: 119-127.

46. Peker S. Radyocerrahi. (Radiosurgery) Aksoy K (ed.), Temel Nörosirurji. Ankara: TND Yayinlari. 2005; 836-843.

47. Goetsch SJ. Risk analysis of Leksell Gamma Knife Model C with automatic positioning system. Int J Radiat Oncol Biol Phys. 2002; 52: 869-877.

48. Horstmann GA, Van Eck AT. Gamma knife model C with the automatic positioning system and its impact on the treatment of vestibular schwannomas. J Neurosurg. 2002; 97: 450-455.

49. Kuo JS, Yu C, Giannotta SL, Petrovich Z, Apuzzo MLJ. The Leksell Gamma Knife Model U versus Model C: A quantitative comparison of radiosurgical treatment parameters. Neurosurg. 2004; 55: 168-172.

50. Régis J, Hayashi M, Porcheron D, Delsanti C, Muracciole X, Peragut JC. Impact of the model C and Automatic Positioning System on gamma knife radiosurgery: an evaluation in vestibular schwannomas. J Neurosurg. 2002; 97: 588-591.

51. Tlachacova D, Schmitt M, Novotny J Jr, Novotny J, Majali M, Liscak R. A comparison of the gamma knife model C and the automatic positioning system with Leksell model B. J Neurosurg. 2005; 102: 25-28.

52. Flickinger JC, Lunsford LD, Kondziolka D, Maitz A. Potential human error in setting stereotactic coordinates for radiosurgery: implications for quality assurance. Int J Radiat Oncol Biol Phys. 1993; 27: 397-401.

53. Kondziolka D, Maitz AH, Niranjan A, Flickinger JC, Lunsford LD. An evaluation of the Model C gamma knife with automatic patient positioning. Neurosurgery. 2002; 50: 429-431.

54. Levivier M, Goldman S, Bidaut LM, Luxen A, Stanus E, Przedborski S, Balériaux D. Positron emission tomography-guided stereotactic brain biopsy. Neurosurgery. 1992; 31: 792-797.

55. Levivier M, Goldman S, Pirotte B, Brucher JM, Balériaux D, Luxen A, Hildebrand J. Diagnostic yield of stereotactic brain biopsy guided by positron emission tomography with [18F]fluorodeoxyglucose. J Neurosurg. 1995; 82: 445-452.

56. Levivier M, Wikler D, Goldman S, Pirotte B, Brotchi J. Positron emission tomography in stereotactic conditions as a functional imaging technique for neurosurgical guidance. Alexander EB III, Maciunas RM, editors. In: Advanced Neurosurgical Navigation. New York, NY: Thime Medical Publishers, Inc: 1999; 85-99.

57. Levivier M, Wikler D Jr, Massager N, David P, Devriendt D, Lorenzoni J, et al. The integration of metabolic imaging in stereotactic procedures including radiosurgery: a review. J Neurosurg. 2002; 97: 542-550.

58. Levivier M, Massager N, Wikler D, Lorenzoni J, Ruiz S, Devriendt D, et al. Use of stereotactic PET images in dosimetry planning of radiosurgery for brain tumors: clinical experience and proposed classification. J Nucl Med. 2004; 45: 1146-1154.

59. Kondziolka D. Gamma knife thalamotomy for disabling tremor. Arch Neurol. 2002; 59: 1660.

60. Ohye C, Shibazaki T, Sato S. Gamma knife thalamotomy for movement disorders: evaluation of the thalamic lesion and clinical results. J Neurosurg. 2005; 102: 234-240.

61. Liscák R, Vladyka V, Simonová G, Vymazal J, Novotny J Jr. Gamma knife radiosurgery of the brain stem cavernomas. Minim Invasive Neurosurg. 2000; 43: 201-207.

62. Pollock BE, Garces YI, Stafford SL, Foote RL, Schomberg PJ, Link MJ. Stereotactic radiosurgery for cavernous malformations. J Neurosurg. 2000; 93: 987-991.

63. Zhang N, Pan L, Wang BJ, Wang EM, Dai JZ, Cai PW. Gamma knife radiosurgery for cavernous hemangiomas. J Neurosurg. 2000; 93: 74-77.

64. Kondziolka D, Lunsford LD, Flickinger JC, Kestle JR. Reduction of hemorrhage risk after stereotactic radiosurgery for cavernous malformations. J Neurosurg. 1995; 83: 825-831.

65. Hasegawa T, McInerney J, Kondziolka D, Lee JY, Flickinger JC, Lunsford LD. Long-term results after stereotactic radiosurgery for patients with cavernous malformations. Neurosurgery. 2002; 50: 1190-1197.

66. Kida Y, Hasegawa T. Radio surgery for cavernous malformations: Results of long term follow up. Kondziolka D. In: Radio surgery. Basel: Karger. 2004; 153-160.

67. Nagy G, Razak A, Rowe JG, Hodgson TJ, Coley SC, Radatz MW, et al. Stereotactic radiosurgery for deep-seated cavernous malformations: a move toward more active, early intervention. Clinical article. J Neurosurg. 2010; 113: 691-699.

68. Lee CC, Pan DH, Chung WY, Liu KD, Yang HC, Wu HM, et al. Brainstem cavernous malformations: the role of Gamma Knife surgery. J Neurosurg. 2012; 117: 164-169.

69. Chang SD, Levy RP, Adler JR Jr, Martin DP, Krakovitz PR, Steinberg GK. Stereotactic radiosurgery of angiographically occult vascular malformations: 14-year experience. Neurosurgery. 1998; 43: 213-220.

70. Huang YC, Tseng CK, Chang CN, Wei KC, Liao CC, Hsu PW. LINAC radiosurgery for intracranial cavernous malformation: 10-year experience. Clin Neurol Neurosurg. 2006; 108: 750-756.

71. Karlsson B, Kihlström L, Lindquist C, Ericson K, Steiner L. Radiosurgery for cavernous malformations. J Neurosurg. 1998; 88: 293-297.

72. Kim DG, Choe WJ, Paek SH, Chung HT, Kim IH, Han DH. Radiosurgery of intracranial cavernous malformations. Acta Neurochir (Wien). 2002; 144: 869-878.

73. Pollock BE, Garces YI, Stafford SL, Foote RL, Schomberg PJ, Link MJ. Stereotactic radiosurgery for cavernous malformations. J Neurosurg. 2000; 93: 987-991.

74. Lee JH, Im YS, Kim JS, Hong SC, Lee JI. Gamma knife radiosurgery of the brain stem cavernous angioma. Korean J Cerebrovasc Surg. 2008; 10: 323-328.

75. García Muñoz L, Velasco Campos F, Lujan Castilla P, Enriquez Barrera M, Cervantes Martínez A, Carrillo-Ruiz J. Radiosurgery in the treatment of brain cavernomas. Experience with 17 lesions treated in 15 patients. Neurochirurgie. 2007; 53: 243-250.

76. Azimi P, Shahzadi S, Bitaraf MA, Azar M, Alikhani M, Zali A, et al. Cavernomas: Outcomes after gamma-knife radiosurgery in Iran. Asian J Neurosurg. 2015; 10: 49.

77. Amin Hanjani S, Ogilvy CS, Candia GJ, Lyons S, Chapman PH. Stereotactic radiosurgery for cavernous malformations: Kjellberg's experience with proton beam therapy in 98 cases at the Harvard Cyclotron. Neurosurgery. 1998; 42: 1229-1236.

78. Karlsson B, Tsai YT. Radiosurgery for cavernomas – A Meta analysis. Pan Arab J Neurosurg. 2009; 3: 36-42.

79. Kida Y, Hasegawa T, Iwai Y, Shuto T, Satoh M, Kondoh T, et al. Radiosurgery for symptomatic cavernous malformations: A multi-institutional retrospective study in Japan. Surg Neurol Int. 2015; 6: S249-257.